CHALMERS
UNIVERSITY OF TECHNOLOGY

Dynamics of particle cloud in stirred vessels

Master of Science Thesis in the Master Degree Program:

Innovative and Sustainable Chemical Engineering

RASMUS JONSSON

Department of Chemical and Biological Engineering
CHALMERS UNIVERSITY OF TECHNOLOGY
Gothenburg, Sweden 2014

Dynamics of particle cloud in stirred vessels

Master of Science Thesis in the Master Degree Program: Innovative and Sustainable Chemical Engineering

RASMUS JONSSON

Department of Chemical and Biological Engineering

Chalmers University of Technology

SE-412 96 Göteborg

Sweden

Telephone + 46 (0)31-772 1000

Abstract

Mixing of different compounds is a common operation in the chemical industry. Two recurrent processes where mixing is essential is crystallization and catalytic reaction. These are often operated in a stirred vessel with a solid phase consisting of particles and a continuous phase. The behavior of the particles in these systems is of utmost importance and is therefore of interest to study. This work is focused on the dynamics of the particle cloud in stirred mixing vessels. The study aims to find the variables affecting the particle cloud height and the periodic behaviors of the particle cloud.

Numerous experiments were conducted on a water filled glass vessel with particles present. The vessel was recorded by a video camera and post processed in Matlab R2013b. The studied variables were the particle size, the impeller speed and the particle loading. Data from four simulations, using computational fluid dynamics (CFD), were compared with the results from the experiments.

Results from the experiments show that the average particle cloud height is linearly dependent on both impeller speed and particle loading. The average cloud height increased with an increasing impeller speed and a decreasing particle load. For a decreasing particle size the average cloud height increased and the standard deviation of the cloud height decreased.

Two dominant frequencies were found in the particle cloud. One had a Strouhal number in an interval of 0.015-0.03. This frequency was dominant in all experimental cases and was unaffected by the change in the variables examined. It existed in all examined locations in the mixing vessel. The other frequency had a Strouhal number of 0.045-0.06. This frequency show close connections to the macro instability (MI) in the continuous phase. As the particle loading increased the energy of the frequency decreased. Furthermore, the energy of the frequency was shown to be locally dependent in the vessel. It was found stronger further down in the vessel and closer to the windward side of the baffle.

Acknowledgement

I want to give thanks to Matthias Eng and Anders Rasmuson for the help and guidance during my master thesis work. They have been there for discussing ideas and taken the time for me when I needed it. Their positive attitude has made this a memorable part of my education and I am thankful for it. Furthermore I would like to thank my fellow master thesis students for the good time spent together and shared laughs.

Nomenclature

MI	Macro instability
S	Strouhal number
f	Frequency of dissipating vortexes, Hz
L	Characteristic length, m
V	Velocity of main flow, m/s
$f_{impeller}$	Frequency of impeller, Hz
Re	Reynolds number
Re_p	Reynolds particle number
PBT	Pitch blade turbine
C_d	Drag coefficient
A	Cross-sectional area, m^2
ρ_f	Density of fluid, kg/m^3
ρ_r	Relative density, kg/m^3
u_r	Relative velocity, m/s
g	Gravity constant, m/s^2
V_p	Volume of particle, m^3
N_c	Critical frequency, Hz
K	Zwietering constant
X	Weight percentage
d_p	Particle diameter, m
v	Kinematic viscosity, m^2/s
D	Impeller diameter, m
T	Vessel diameter, m
C	Impeller clearance, m
B	Baffle width, m
H	Liquid height in vessel, m
N_i	Impeller frequency, m
μ_f	Dynamic viscosity for continuous phase, (kg m)/s
St	Stokes number
St_{coll}	Stokes collisional number
τ_{ex}	Particle response time, s
τ_f	Time scale of continuous phase, s
τ_{coll}	Time scale of particle-particle collisions, s
τ	Time step, s
ω	Angular frequency, 1/s
t	Time for measure points, s
N	Number of data
h	Measured value
$\bar{h}$	Mean of measured values
σ	Variance of measured values
P_N	Energy fraction
CFD	Computational fluid dynamics
LES	Large eddy simulation
LPT	Lagrangian particle tracking
S_1	Frequency within given interval
S_2	Frequency within given interval

Contents

1. Introduction

A common operation in the chemical industry is mixing of two phase systems. Two operations which contain mixing of two phases are crystallization and catalytic reaction. Both mix a solid phase with a continuous phase and the mixing is mostly carried out in stirred vessels with high particle loading. Numerous studies of a single phase system in stirred vessels exist and the behavior of the continuous phase is well known [1] [2] [3]. Since it is common with two phase systems there are several studies on the continuous phase when particles are present in vessel [4] [5]. These normally focus on how the particles affect the continuous phase. Only a few studies are focusing on the particle dynamics in the vessel [5].However, in industry the particle behavior is of utmost importance e.g. in crystallization processes where the particles are the product from the operation hence it is highly motivated to study the particle behavior.

This study aims to describe the dynamic behavior of particles in a stirred vessel. A series of experiments will be conducted on a stirred vessel with particles present. Data from different simulations will be studied and compared to the experimental results. Large particles form a dilute and a dense region in the vessel. The interface between the diluted and the dense region is referred to as the particle cloud height. At the cloud height local measurement of the height and the periodic behavior will be performed. The periodic behavior of particles inside the dense region will be studied to find patterns between continuous phase and particles.

1.1 Macro instability

The flow in the vessel contains motions directly connected to the impeller and low frequency periodic instabilities. The low frequency is often referred to as macro instability (MI) and is generated from the disturbance in the flow caused by baffles. Baffles create areas in the continuous phase where the axial velocity of the fluid is zero. In adjacent zones to the stagnated areas the velocity gradient determines the frequency of the low periodic instability [6] [7]. The frequency of MI is found to always be proportional to the impeller speed. The frequency depends on impeller type, impeller clearance from the bottom of vessel, number of baffle and baffle size.

Experiments have been conducted by *Eng et al.* on the continuous phase for a vessel with same the geometry as the vessel which is used in this study [4]. Velocity changes in the fluid were measured and translated into frequencies using Laser Doppler Velocimetry (LDV). LDV uses two intersecting laser beams and as a particle on the micro-scale level passes through the intersection its velocity can be measured. Particle on the micro-scale level are too small to affect the flow patterns in the continuous phase and therefore the periodic behaviors in the continuous phase will be measured [8]. Picture Image Velocimetry (PIV) is another way to determine periodic behaviors in the continuous phase. Compared to LDV, velocities of particles in a surface are studied using two laser pulses rather than an intersection between two lasers [8]. Continuous phase contains frequencies of the MI and the impeller with its higher modes. These higher modes of the impeller originate from the number of blades on the impeller and this is visualized in Figure 1.1 which is from the article by *Eng et al.* and shows an energy spectrum from the continuous phase for a position located close to the impeller.

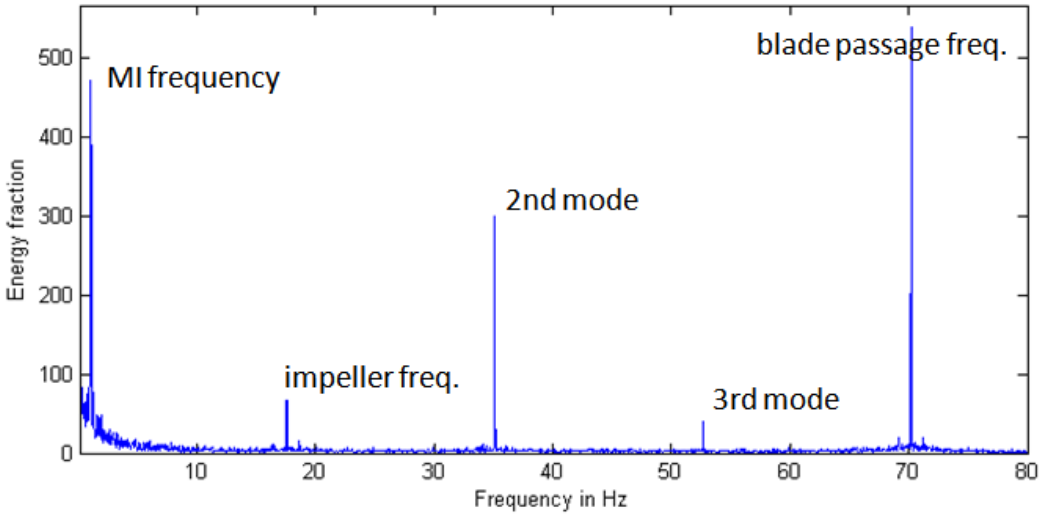

Figure 1.1: Energy containing frequencies of the continuous phase in a stirred vessel [4]

The MI is proportional to the impeller frequency and is therefore normally mention in terms of a dimensionless frequency, a ratio between the MI and the impeller frequency. Strouhal number is often used to describe dimensionless frequencies in stirred vessels. The Strouhal number is defined as:

$$S = \frac{fL}{V} \tag{1}$$

In a simplified way the Strouhal number describes the ratio of frequencies in the flow compared to a generating source. For stirred vessels the impeller is the generating source. The Strouhal number is therefore redefined as the ratio between frequencies in the flow and the impeller speed. Hence the Strouhal number is defined as:

$$S = \frac{f}{f_{impeller}} \tag{2}$$

Several dimensionless frequencies are stated for the MI. *Hasal et al.* stated S= 0.057 at Re=75000 with a six bladed PBT with an angle of 45^{o} [9].A different Strouhal number is stated by *Eng et al.* for a four bladed PBT with an angle of 45^{o}, the value found in the studies was S= 0.06 at Re= 18000-84000 [4].Studies by *Nikiforaki et al*. shows that S=0.017 for PBT and S= 0.01-0.02 for Rushton turbines. It is found in the same studies that the Strouhal number is locally dependent at low Reynolds numbers [10]. The difference in the reported Strouhal numbers shows that MI is strongly dependent on geometry.

1.2 Particle Cloud Height

There is a formation of a particle cloud in stirred vessels when large enough particles are present. The top of the cloud is located at a position where raising and falling particles meet. At this position the kinetical energy introduced by the impeller and the potential energy caused by the gravitational force is evened out. There are two dominant forces acting on a particle in a mixing vessel, drag force and gravity. General equations for the drag force and the gravitational force follows:

$$Drag\ force = \frac{1}{2} C_d A \rho_f {u_r}^2 \quad (3)$$

$$Gravitational\ force = \rho_r g V_p \quad (4)$$

In the equations A is the cross-sectional area of the solid and V_p is the volume of the particle. Both depend on the particle diameter which makes it an important parameter in system. The potential energy of a particle is the gravitational force multiplied with the height of the particle and is therefore dependent on the particle size as well.

A study has shown that the MI is dampened out in the diluted regime above the particle cloud height [5]. The experiments were conducted with a volume fraction of 11%vol and 0.3 mm particles. However, another study indicates that the MI exists at strong energy levels above the cloud height for volumetric concentrations up to 11.8%vol and particle sizes of 1, 1.5 and 2 mm [4].These two studies raise the debate of the impact of the discrete phase on continuous phase.

Zwietering published an article in 1958 where he conducted numerous experiments on stirred vessels with particles present. This resulted in a correlation for the critical frequency which is the frequency of the impeller when all particles are suspended in the vessel [11]. While the impeller frequency is below the critical frequency some particles will be in rest on the bottom of the vessel. To reach the critical frequency is important for industrial processes since particles in rest on the bottom have less contact surface with the continuous phase.

For systems with 20 weight-percentages of particles or less, the correlation given by Zwietering follows:

$$N_c = K \left(\frac{g \rho_r}{\rho_f} \right)^{0.45} \frac{X^{0.13} d_p^{0.2} v^{0.1}}{D^{0.85}} \quad (5)$$

The correlation of the critical frequency depends on the density of phases, weight-percentage, particle diameter, kinematic viscosity, impeller diameter and a constant which depends on impeller type and the ratio of T/C. All variables in the correlation are important for lifting particles from the bottom of a vessel. However, the correlation gives the critical frequency but no information about the cloud height in the vessel.

The cloud height is often simplified in studies by averaging over the whole vessel. *G.Micale et al.* showed that the average height over the whole vessel is linearly dependent on impeller speed. CFD simulation results were compared with visual observation of the cloud height [12]. An error of 5% was estimated for the cloud height in the observations.

2 Experiments

Two approaches are used to analyze the behavior of the particle cloud, a larger experimental part and a smaller simulation part to compare with the experimental results. The simulations are performed by *Eng.M* but the treatment of data from the simulations is a part of this study.

2.1 Experimental Setup

The equipment used for the experiments has the same geometry as *Eng et al*. used for studying the MI-phenomenon [4]. A flat bottom glass vessel with a diameter of T=15 cm and 4 baffles with a width of B=1 cm is used for the experiments. The tank is filled with water to a height of H=T. A 45° 4 bladed PBT-impeller is used with D=5 cm. The bottom clearance for the impeller is C=T/3. Spherical glass particles with a density of 2.5 kg/m^3 and 3 different diameters (2mm, 1mm and 0.5 mm) are used.

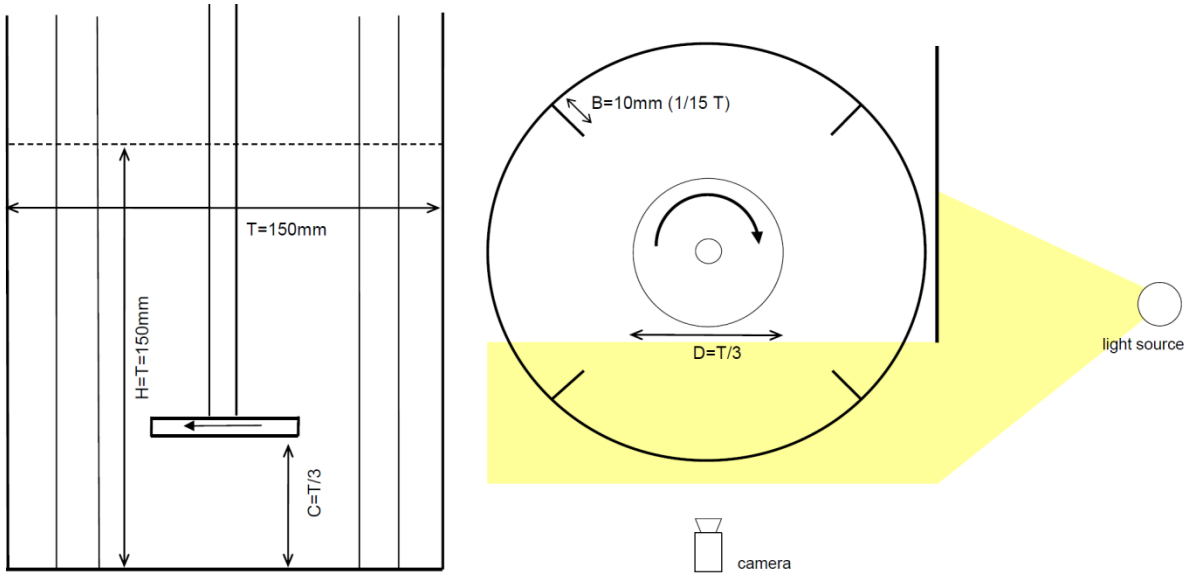

Figure 2.1: The dimensions of the vessel and experimental setup.

The region of interest in the vessel is between the baffles due to the disturbance in the flow generated by the baffles. A lamp lightens this region while the remaining part is kept dark by a screen. A camera is placed in front of the vessel according to figure 2.1 to capture the reflections from the particles in the lightened area. Each case is recorded for 30 seconds with 25 fps which leaves 750 frames per case. Experiments are conducted according to table 1.1.

Table 1.1: The experimental setup of cases

	2,5 %vol	5 %vol	7,5 %vol	10 %vol	15 %vol	20 %vol
0,5 mm	20	20	25	25	27,5	--
	25	25	27,5	27,5	30	--
	27,5	27,5	30	30	32,5	--
	30	30	32,5	32,5	35	--
1 mm	20	20	25	25	27,5	30
	25	25	27,5	27,5	30	32,5
	27,5	27,5	30	30	32,5	35
	30	30	32,5	32,5	35	37,5
2 mm	20	20	25	25	27,5	30
	25	25	27,5	27,5	30	32,5
	27,5	27,5	30	30	32,5	35
	30	30	32,5	32,5	35	37,5

Variables chosen for the experiments are based on the Zwietering equation. These variables are volume fraction, particle diameter and impeller speed. Impeller speed is proportional to the Reynolds number of the vessels which is defined by equation 5. The Reynolds number in the experiments ranges from 50000 at 20 Hz of impeller speed to 94000 at 37.5 Hz of impeller speed. Only the continuous phase is considered in the Reynolds number and the system is considered turbulent at approximately Re=10000

$$Re = \frac{N_i D^2 \rho_f}{\mu_f} \tag{6}$$

Stokes number indicates if the particle motion is mostly governed by interaction with continuous phase or particle-particle interaction and is therefore an important tool in multiphase systems. The Stokes number depends on the particle response time, the time scale of the continuous phase and the time scale of particle-particle collisions. Rough estimations of the Stokes numbers can be made by assuming $Re_p<1$ which makes equation 7 valid for the particle response time.

$$\tau_{ex} = \frac{\rho_p d_p^2}{18\mu_f} \tag{7}$$

$$St = \frac{\tau_{ex}}{\tau_f} \tag{8}$$

$$\mathrm{St_{coll}} = \frac{\tau_{\mathrm{ex}}}{\tau_{\mathrm{coll}}} \tag{9}$$

Both τ_f and τ_{coll} are difficult to estimate which makes the Stokes numbers in equation 8-9 difficult to solve but for a given value of Stokes number both τ_f and τ_{coll} can be estimated. In table 2.1 values have been set to St=1 and St_{coll} =1 which is the threshold in both equations.

Table 2.1: Values for τ_f and τ_{coll} with St=1, St_{coll} =1, μ=1x10^{-3}, ρ=1x10^{3}

Particle diameter	2 mm	1 mm	0.5 mm
$^1/_{\tau_f}$ and $^1/_{\tau_{coll}}$	1.818 Hz	7.2 Hz	28.8 Hz

For frequencies in the continuous phase higher than frequencies in table 2.1 particles will not match changes in the continuous phase accurately. For collisional frequencies larger than the values in table 2.1 the system is considered dense. The values in the table are very rough due to the assumption of Re_p<1. However it is reasonable to assume that particles will follow the MI in most of the experimental cases and that the system will be dense in all experimental cases hence particle-particle interactions are of utmost importance in the particle cloud.

2.2 Post Processing

Matlab R2013b is used to analyze the frames from the experiments. The resolution of each frame is 1080x1920 pixels which captures single particles and is therefore well suited for the post processing. Figure 2.2 is an original frame before any picture manipulation. Single particles are visible and the reflections of particles outside of the region of interest are negligible.

Figure 2.2: A frame before any light-scale manipulation from the 1mm diameter, 10%vol and 32.5 Hz case

Two methods for measuring the dynamic behavior of the particle cloud are used. These methods are visualized in figure 2.4 and are referred to as method A and method B. Method A measures the cloud height directly by counting pixels from the top of the vessel until the cloud height is reached. By repeating the procedure for all frames a temporal resolution of height versus time is generated. The light scales of the frames are adjusted so particles outside the region of interest appear black while the particles inside the region are brightened. The contrast adjustment can be seen by comparing figure 2.2 and figure 2.4. The code requires 200 non-black pixels (approximately 2 cm) in a row as a threshold to accept the position of the cloud height. This threshold filters out single particles in the upper dilute region of the vessel hence the cloud height will, due to the threshold, be measured at the position where the dense region starts. For this method, four positions are chosen such that a wider range of the particle cloud is measured. Three positions are located on the windward baffle side due to the disturbance generated on the continuous phase from the baffle. The last one is located on the leeward baffle side. The positions can be seen in figure 2.3 and are marked as H1-H4.

Method B estimates the brightness in the same area in each frame and is visualized in figure 2.4. The brightness in the chosen area is connected to the particle density. Hence the method generates a temporal resolution of concentration versus time. The strength of this approach is in comparison to method A the possibility to measure changes inside the particle cloud. However, it is more dependent on positioning of the light source. To generate a sufficient overlook of the particle cloud behavior 9 positions are analyzed. These positions are spread from half of the liquid height (7.5 cm) to 5/6 of the liquid height (12.5 cm). The areas are divided into 3 columns with 3 rows in each and are visualized in Figure 2.3.

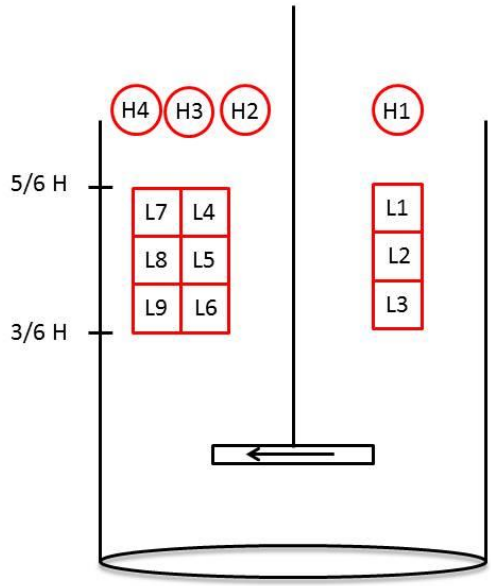

Figure 2.3: Locations where measurements are taken. H1-H4 are the positions for method A and L1-L9 are the positions for method B.

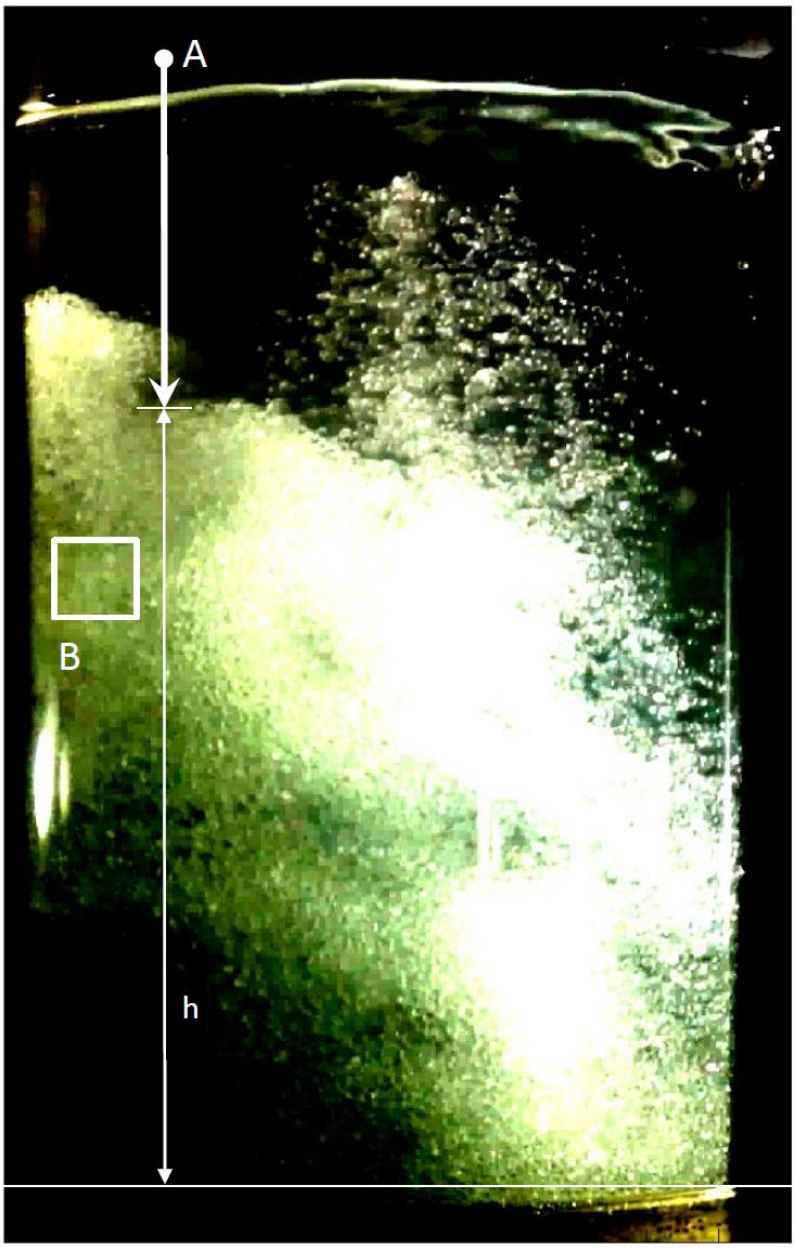

Figure 2.4: Instantaneous picture of the vessel with light-scale manipulation. Method A and method B are graphically visualized

2.3 Lomb Algorithm

Both methods generate fluctuating data which can be described in frequencies. To analyze frequencies it is common to use either Fourier transforms or Lomb algorithm. Fourier Transform is less computational heavy but demands evenly spaced data. The Lomb algorithm is more computational heavy and can handle unevenly spaced data. Frames from the videos are evenly spaced which means that both approaches are valid. In the study, Lomb algorithm is used for the frequency analysis since a Matlab-code is already available making it a more convenient choice.

Lomb algorithm uses a “per point “approach instead of “per time” approach of the given data. The constant time step used is defined by equation 10.

$$\tan 2\omega\tau = \frac{\sum_j \sin 2\omega t_j}{\sum_j \cos 2\omega t_j} \tag{10}$$

The mean value and the variance of the N data points are calculated from equation11-12.

$$\bar{h} = \frac{1}{N}\sum_{1}^{N} h_i \tag{11}$$

$$\sigma^2 = \frac{1}{N-1}\sum_{1}^{N}\left(h_i - \bar{h}\right)^2 \tag{12}$$

With given equations, the energy spectra, P_N, can be calculated as a function of the angular frequency, ω, and is defined by equation 13.

$$P_N(\omega) = \frac{1}{2\sigma^2}\left(\frac{\left(\sum_j (h_j - \bar{h})\cos\omega(t_j - \tau)\right)^2}{\sum_j \cos^2\omega(t_i - \tau)} + \frac{\left(\sum_j (h_j - \bar{h})\sin\omega(t_j - \tau)\right)^2}{\sum_j \sin^2\omega(t_j - \tau)}\right) \tag{13}$$

The code used for solving the Lomb algoritm is a translation in to Matlab from *Numerical recipies in C* where the code is written in C-language [13].An example of the Lomb algoritm is visualized in figure 2.5. The temporal information of the cloud height is converted into a energy spectrum. The energy fraction, or amplitude, of a frequeny corresponds to its consistency in the given data. A consisten frequency is clear over the whole time interval with a small or negligible deviation.

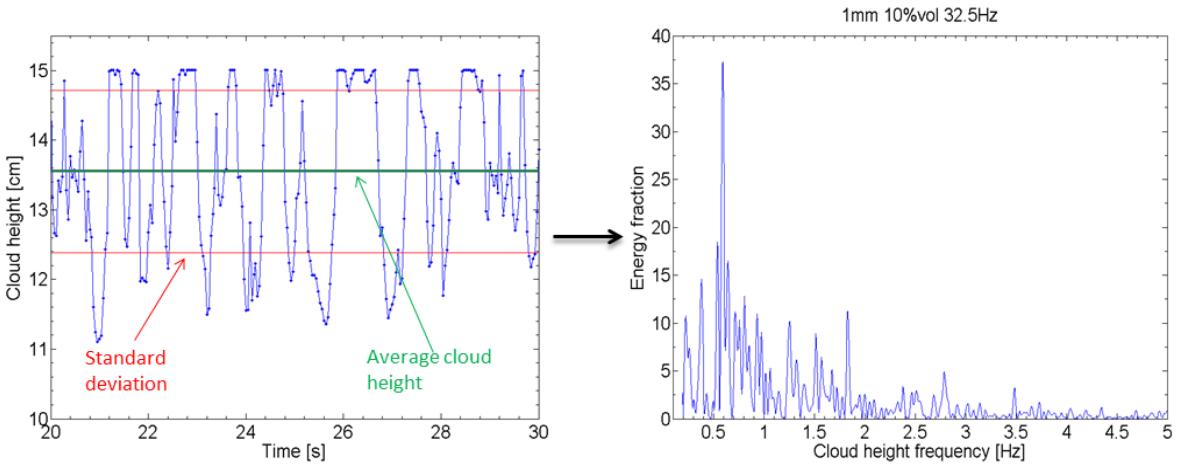

Figure 2.5: Demonstration of the Lomb algorithm for the 1mm diameter, 10%vol, 32.5 Hz case

2.4 Cloud Height

A method similar to method A mentioned under the post processing is used to measure the changes in the cloud height. To convert the cloud height position from pixels to real length scales the liquid surface height is averaged in each video. Information of the pixel distance between top and bottom of the vessel enables the cloud height to be converted into real length scales. The temporal resolution of height versus time is averaged for all cases. The surface height is only measured from position “H3” in figure 2.3.

2.5 CFD Modelling

As a complement to the experiments, 4 cases are simulated using ANSYS Fluent 14.5. The continuous phase is solved with Large Eddy Simulation (LES) and the discrete phase is solved with Lagrangian Particle Tracking (LPT). LES demands a fine mesh to accurate resolve the turbulence in the flow field. In opposite to LES, LPT needs a course grid to maintain a good statistical solution for the particles. This problem is solved by a statistical method implemented in ANSYS Fluent called node based averaging. This method reduces extreme source terms from single particles by averaging them over several neighboring cells. The geometry in the simulations is identical to the vessel used in the experiments.

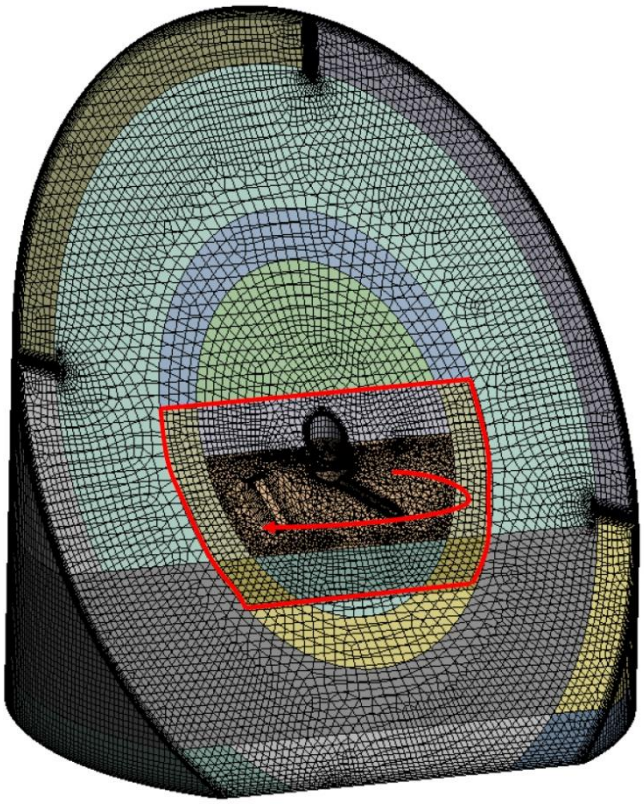

Figure 2.6: The simulations are using a rotating mesh with tetrahedral cells

The cases are simulated with 16 core processors of 3 GHz with a time step of $2x10^{-5}$ [s]. Table 2.3 shows the setup for the cases. Due to the limitations of computational power, the cases containing 1mm particles are reduced to low particle volume fraction.

Table 2.3: the 4 Cases for simulation

	Particle diameter	Impeller frequency	Particle volume%	Number of particles
Case 1	1 mm	20 Hz	1.1852	60000
Case 2	1 mm	30 Hz	1.1852	60000
Case 3	2 mm	30 Hz	5.9733	37800
Case 4	2 mm	30 Hz	9.4815	60000

For every hundredth time step, all particle positions and velocities are saved for post-processing. A Matlab code is developed to be similar to method A. The code introduces a column of computational cells from the top of the vessel at a position close to H3 in figure 2.3. Then it counts all particles in these cells downwards. When all particles in every cell are counted the location of the highest gradient between the cells determines the cloud height. The temporal resolution of the cloud height from the CFD simulations is processed by the Lomb algorithm to detect the dominant frequencies.

3 Results and Discussion

The results and discussions are divided into three parts. In the first part, results from the analysis of the particle cloud height will be discussed and how it is affected by the parameters varied in the experiments. The second part treats periodic behaviors in the particle cloud and how they depend on varied parameters. Furthermore, local differences in the periodic behavior of the particle cloud is analyzed and discussed. In the third part comparisons are made between the simulated cases and the experimental cases.

3.1 Particle Cloud Height

The cloud height is measured in the same location for each experimental case and from the temporal information of the cloud height an averaged value and a standard deviation is determined. Relations between the cloud height and the variables in the experimental setup are determined by graphical solutions.

For each particle size the average cloud height is linearly dependent of the impeller speed. Hence, the average cloud height is linearly dependent of the Reynolds number in equation 6. This result agrees with the experiments by *G.Micale et al*. [12].His result is valid for the average over the whole vessel while these results are valid for a single location. Figure 3.1 shows the average cloud height versus the impeller frequency for each particle diameter at 10 %vol. The particle cloud height increases as the impeller speed increases.

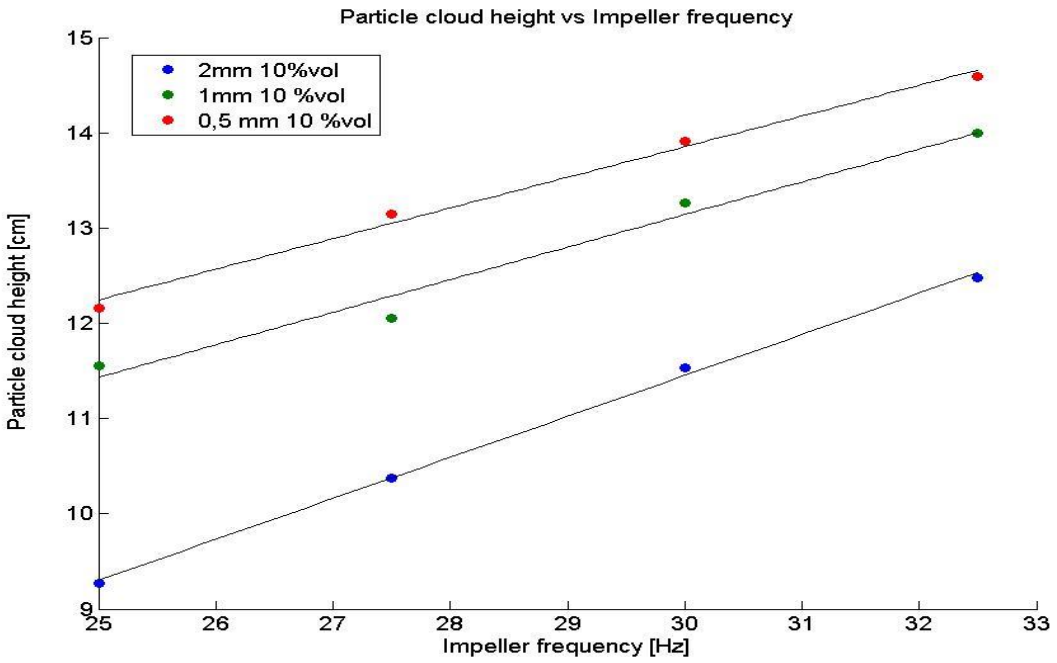

Figure 3.1: Average cloud height vs impeller frequency at 10 %vol. All particle sizes show a linear behavior.

The cloud height is linearly dependent of the volume fraction for all particle diameters studied. With an increasing volume fraction the height decreases. This behavior appears logical since more particles of same size are added to the system which would increase the overall energy to lift the particle cloud. In figure 3.2 the cloud height is plotted against the volume faction at a constant impeller speed.

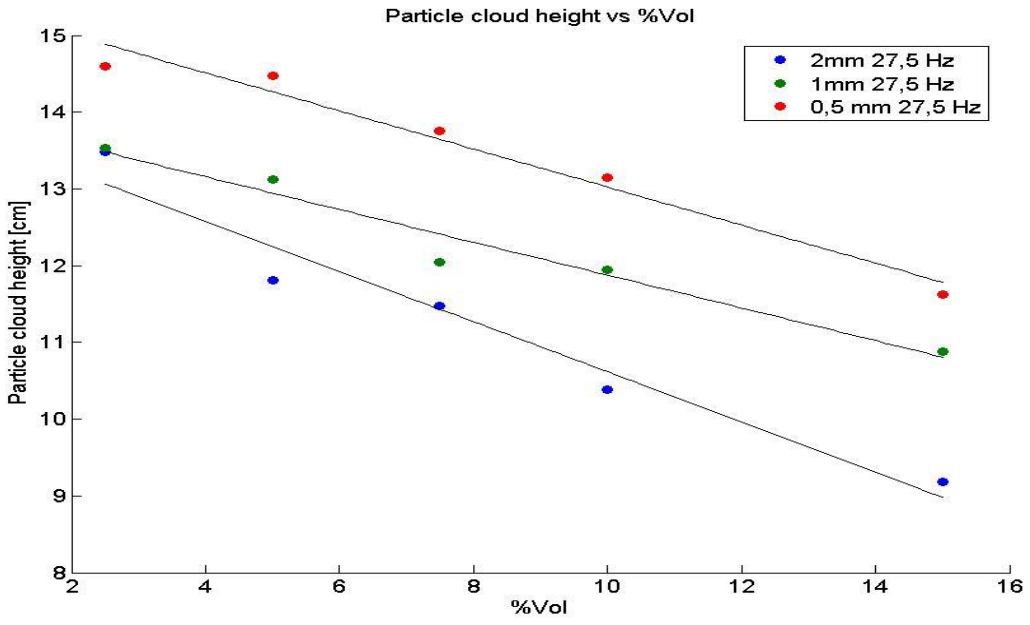

Figure 3.2: Average cloud height vs volume fraction at an impeller speed of 27.5 Hz. All particle sizes show a tendency to linear behavior.

The deviation from the average cloud height differs for each experimental case. A clear dependency of the particle diameter can be seen in the standard deviation. As the diameter decreases the standard deviation decreases. However neither the volume fraction nor the impeller speed has any effect on the standard deviation. Figure 3.3 shows the difference between particle sizes for 7.5%vol and 25 Hz impeller speed. With a decreasing particle diameter the average cloud height increases. The trend is clear but it is not linearly related, this is likely to stem from energy and force balances not being linearly dependent on particle diameter.

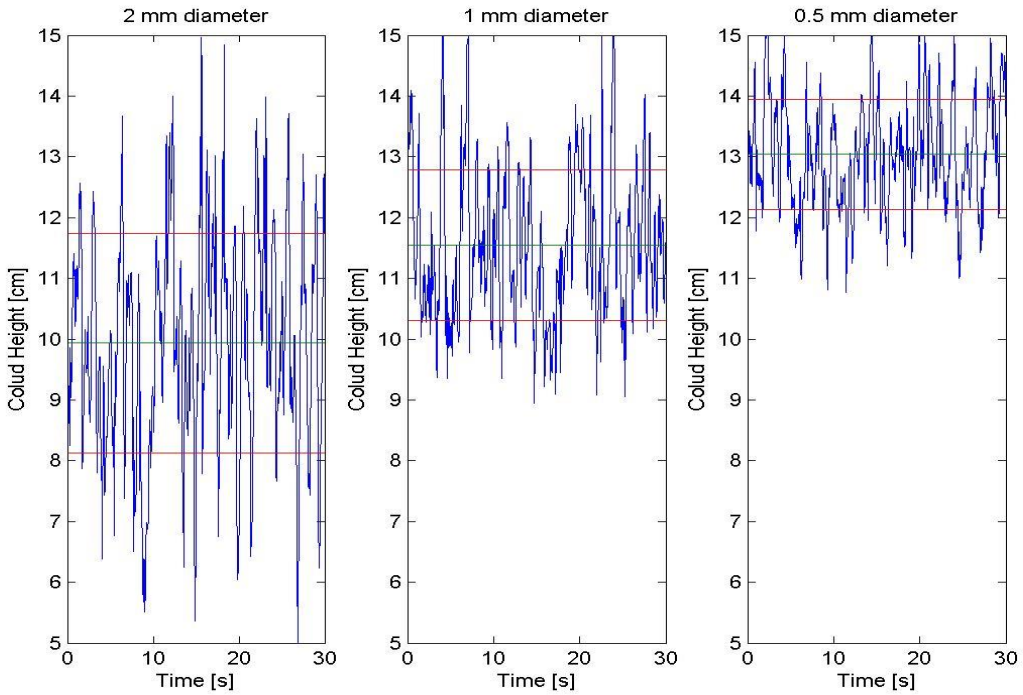

Figure 3.3: A comparison between different particle sizes at 7.5%vol and 27.5 Hz impeller speed. As particle size increases the average cloud height is decreased while the standard deviation of the cloud height is increased.

The standard deviation describes how the cloud height varies in time not how strong the particle cloud is separated from the dilute flow. It could be observed that smaller particles form a less pronounced cloud and more particles will occur dispersed above the identified cloud. Larger particles act exactly opposite to smaller particles, the cloud is very pronounced and only very few particles are dispersed. Figure 3.4 shows the difference in the interface between particle sizes.

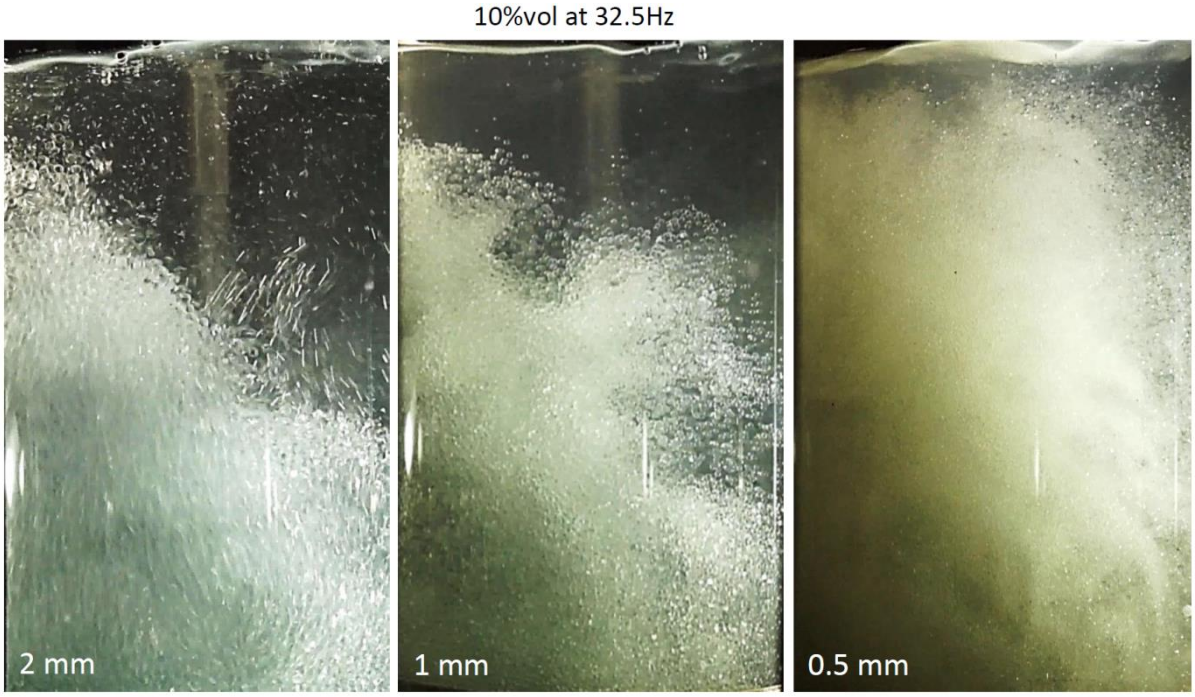

Figure 3.4: Three instantaneous pictures for the different particle sizes. The concentration gradient at the interface between the dilute and the dense region is decreasing as the particle size decreases.

The particle cloud has a dynamic character and is dependent on position in the vessel. The measured height from the post-processing is therefore not valid for the whole tank. Figure 3.5 shows the local differences from position “H3” and “H1” for 10%vol and 32.5 Hz. The cloud height shows strong variations between the different locations.

Information from figure 3.5 weakens the validity of discussing an average cloud height in the whole vessel. Vast local and temporal differences exist in the particle cloud. As the particle size increases the error from the averaging process will increase due to the standard deviation. During averaging processes information will always be lost e.g. the bursts occurring in the middle of the vessel in figure 3.5 is an example of a phenomenon which disappears in the averaging process. Hence, by using several locations less information is lost and the cloud height is described more accurately. In the method used for the post-processing, one single position is used for all cases and therefore it is possibility to determine how the height is affected by the three variables in the experiments.

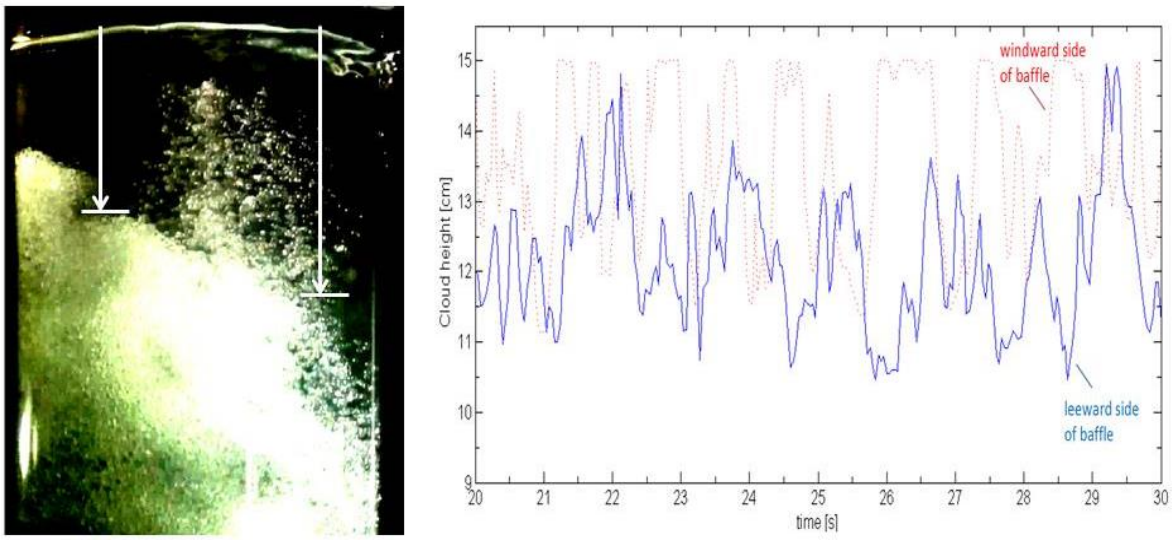

Figure 3.5: Difference between two locations over time. The case is 1mm diameter, 10%vol and 32.5 Hz. The average height is different at different positions in the vessel.

3.2 Particle Frequency

When studying cloud height, the temporal height differences are averaged to achieve a convenient way to describe its behavior. As can be seen in figure 3.5 the height shows a periodic behavior. Using the Lomb algorithm, periodic behaviors can be expressed by an energy spectrum where energy containing frequencies are detected.

In the energy spectra from both methods, two energy containing peaks appear more often than others. One of the energy peaks has a Strouhal number of 0.015-0.03 and the other peak has a Strouhal number of 0.045-0.06, these peaks are referred to as S_1 and S_2 respectively. These peaks are visualized in figure 3.6.

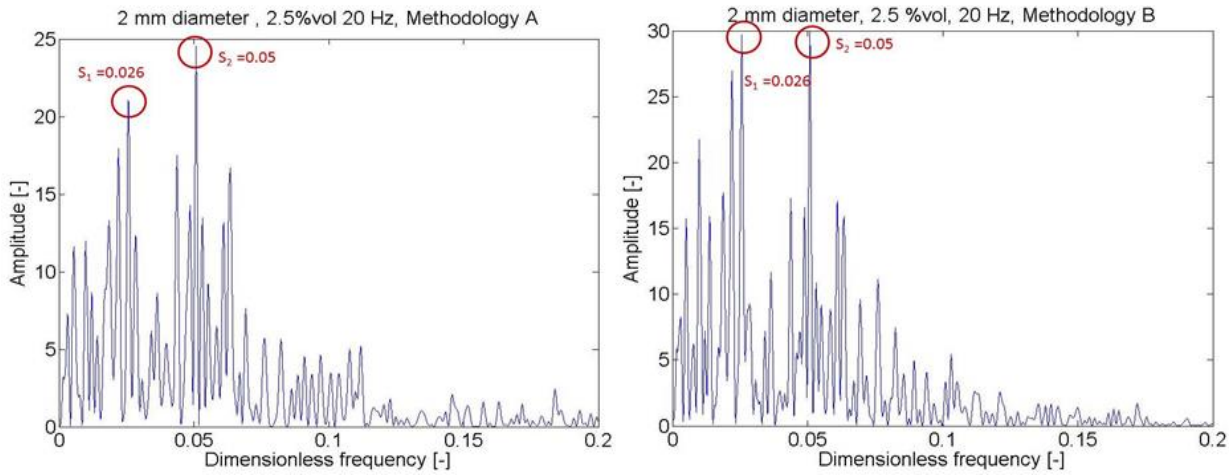

Figure 3.6: Energy spectrum using method A to the left and using method B to the right, both taken from nearby locations in same experimental case. Both methods detect same Strouhal number of the dominant frequencies.

Figure 3.6 shows that both methods give the same peaks which strengthen the reliability in the methods. The Strouhal number for the MI is measured to S=0.06 for a vessel with same geometry as used in the experiments [4] .The interval of S_2 is located close to the MI which makes it reasonable to assume that S_2 is to some extent governed by the MI. However, there is not safe to assume that S_2 is only governed by the MI since the Strouhal number of the MI is constant while S_2 varies.

The strength of method B is the possibility to study a larger area of the particle cloud. From using this method a clear tendency is detected in particle cloud. The tendency shows that independent of location in the cloud, S_1 always exists as an energy containing frequency while S_2 contains more energy further down in the particle cloud and closer to the windward side of the baffle. Assuming S_2 is generated from the MI in the continuous phase this behavior is logical. The MI is strongest close to the baffle where it is generated which would conclude that locations close to the baffle would give more energy to S_2. As particles are added to the system, energy in the continuous phase is consumed by the interactions between particles and continuous phase. At a low position in the vessel less energy is yet consumed from the particle-continuous phase interactions. This behavior agrees with the result from *Bittorf et al*. [5].The MI is stronger and S_2 will be more energy containing further down in the vessel. The local differences are shown in figure 3.7.

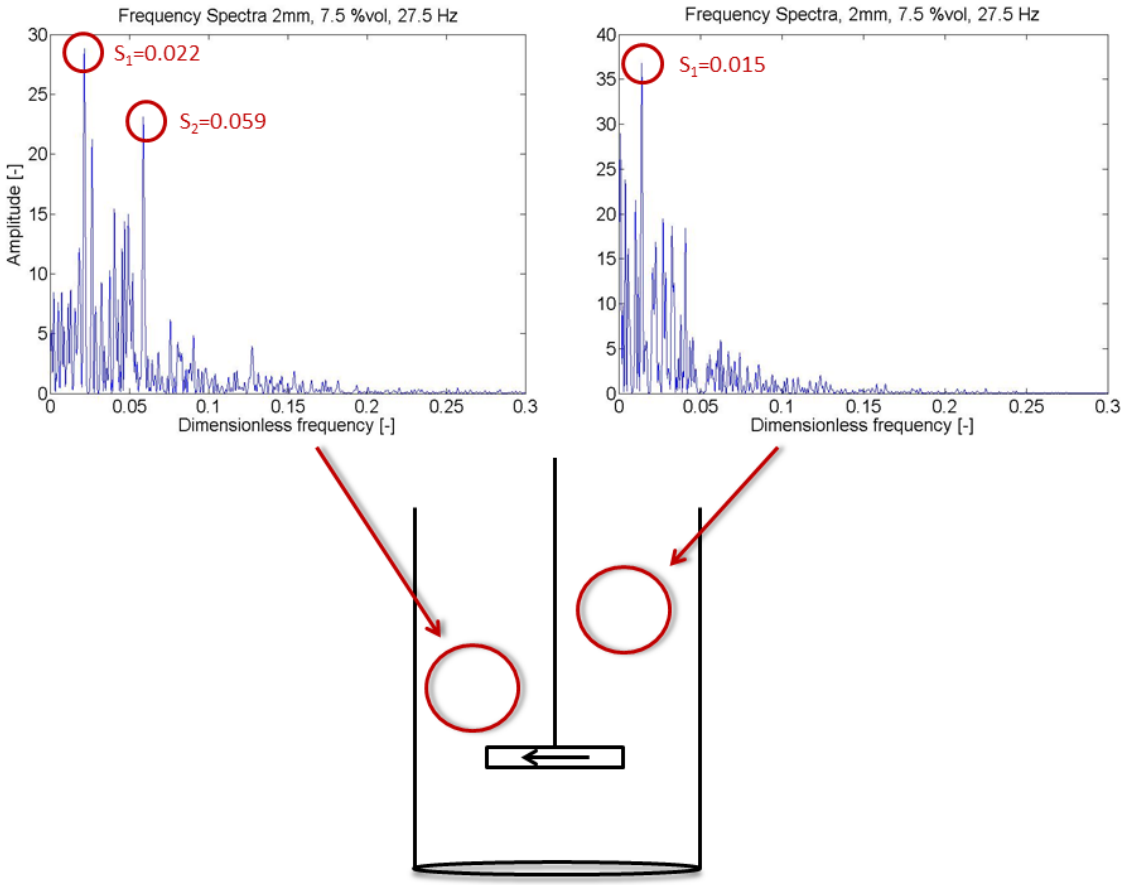

Figure 3.7: Positions in the vessel where S_1 and S_2 are dominating the particle motion

Neither S_1 or S_2 show any dependency of the impeller speed. Both peaks stay within the defined intervals as the impeller speed increases at low volume fractions. In figure 3.8 a comparison is made between the lowest and the highest impeller speed for 2mm diameter and 2.5%vol. The MI for impeller frequencies in the figure is below the value calculated for 2 mm particles in table 2.1. This means, for the assumption of $Re_p<1$ the particles should be able to follow changes in the continuous phase.

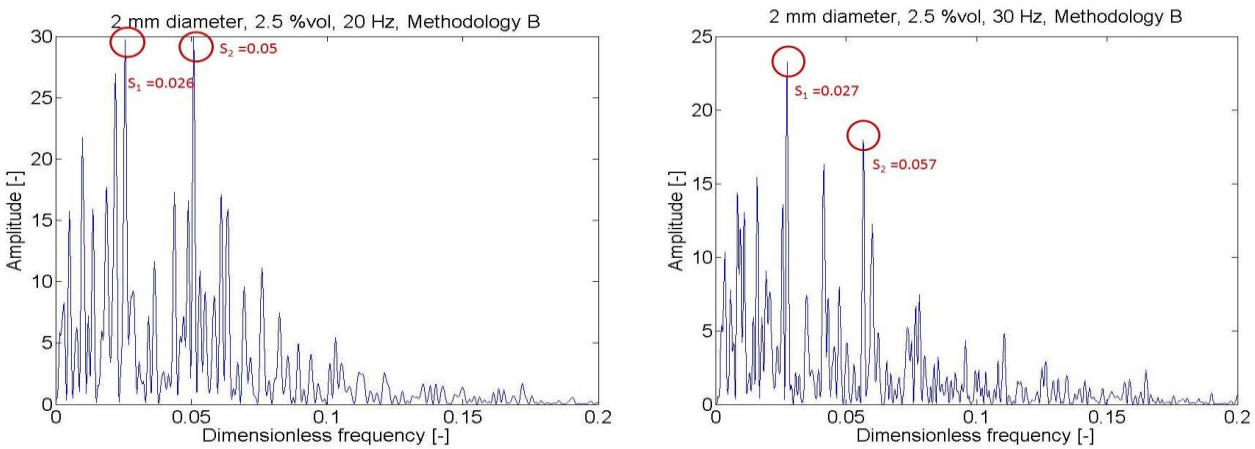

Figure 3.8: Energy spectra for 2mm diameter, 2.5 %vol and 20 Hz and 30 Hz. S_1 changes from 0.026 to 0.027 and S_2 changes from 0.05 to 0.057.

According to the Stokes number calculations, at higher impeller frequencies the 2mm particles will not follow the MI measured by *Eng et al*. in an identical vessel. Figure 3.9 shows the energy spectra for the lowest and the highest impeller speed at 20%vol. It is clear from the figure that S_2 is not energy containing in the 20%vol cases. If only the frequency of the impeller is the limiting factor for the disappearance of S_2 it would be visible in the 1mm and 0.5 mm cases. Other particle sizes show the same behavior as the 2 mm case which rejects the argument of limiting Stokes number. The reason for its disappearance is likely to stem from the high particle loading. A higher particle loading will increased the particle collision frequency hence the particle motions will be more governed by collisions rather than interactions with continuous phase. Motion of particles still originates from continuous phase however due to the dense system particles do not directly follow the continuous phase.

S_1 is clear and dominant for both impeller speeds in figure 3.9. At 37.5 Hz impeller speed S_1 goes outside the defined interval were it generally appears. The different frequencies of S_1 coexists at some locations in the 37.5 Hz case which points towards local differences in the vessel. Anyhow, the Strouhal number 0.026 does exist at the lowest and highest impeller speed for S_1 which implies that it is constant with Reynolds number.

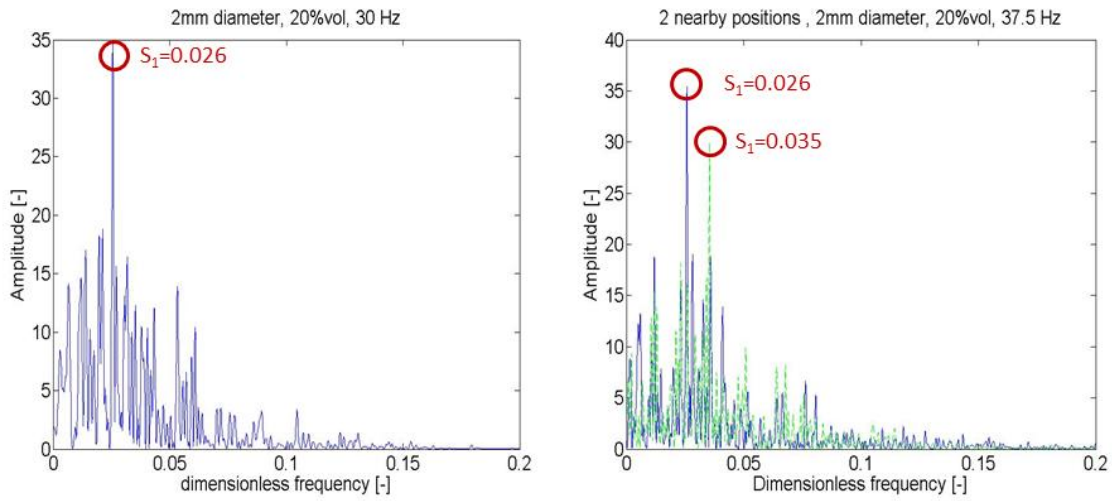

Figure 3.9: Different impeller speeds at 2mm particles and 20%vol. The case with 37.5 Hz impeller speed is plotted with two energy spectra (one is solid blue and on is green dashed) since both is equally common.

The energy, which is the same as the amplitude from the Lomb algorithm, is strongly dependent on the number of measured points and the consistency of the frequencies. The number of measured points affects the amplitude of every frequency in the energy spectra which affects the white noise. Hence, the reasonable way to determine the effect of variables on the amplitude is to compare dominant peaks with surrounding peaks in the energy spectra.

At low volume fractions both S_1 and S_2 are clearly dominant and easy to distinguish from the white noise. When the volume fraction increases the energy of S_2 decreases while the energy of S_1 is stable and slightly increasing. As the volume fraction increases the Stokes number in equation 9 will increase due to shorter time passed between particle collisions. This would strengthen the assumption of S_2 being directly governed by continuous phase. For S_1 the energy is slightly increasing as the volume fraction increases. This would imply that S_1 is to some extent governed by particle-particle interaction since all experimental cases are considered dense in the particle cloud. The changes in S_1 and S_2 for different volume fractions are shown in figure 3.10.

Even if the energy fraction is changed, the Strouhal number of S_1 and S_2 is stable as the particle loading increases. Figure 3.10 shows that the Strouhal numbers stay within the given intervals in which they are defined when the volume fraction increases. The peaks are therefore more dependent on the local position in the mixing vessel than volume fraction.

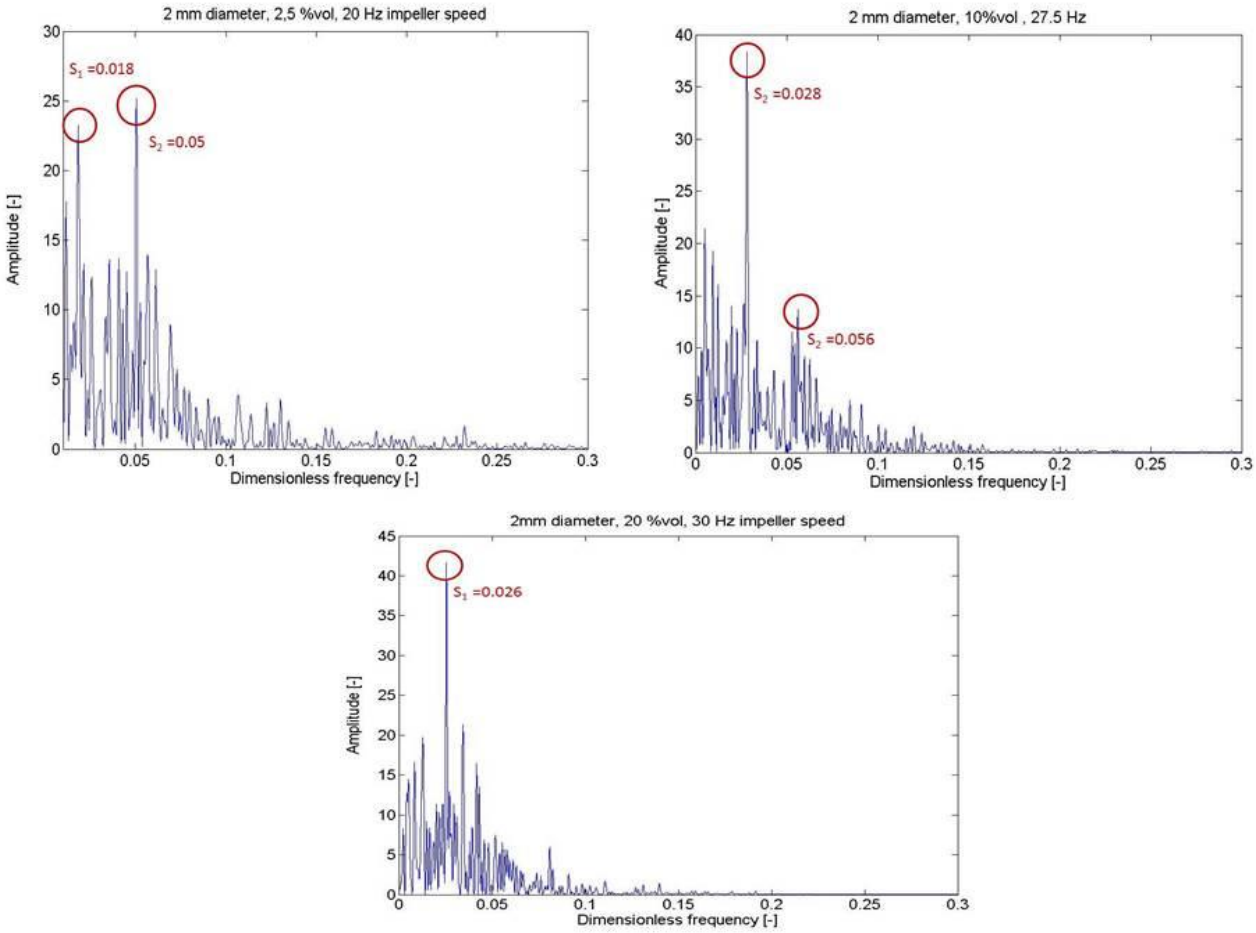

Figure 3.10: The Strouhal number and energy of S_1 and S_2 for 2.5-, 10- and 20%vol

Strouhal numbers for the peaks are shown to be independent of volume fraction which is one of the variables studied in the experiments and no dependency of the impeller speed is seen from the data either. Finally, the remaining variable which could affect the energy spectra of the particles is the diameter. Particle diameter has a strong influence on the fundamental transport equations and the energy balances. Still no tendencies between different particle diameters are seen on S_1 and S_2. Figure 3.11 shows the energy spectrum for all 3 particle sizes with the same volume fraction and impeller speed. The Strouhal number for the frequencies is varying within given intervals. However, 3 diameters are not enough to draw any comprehensive conclusion regarding the effect of the diameter on periodic behavior of the cloud.

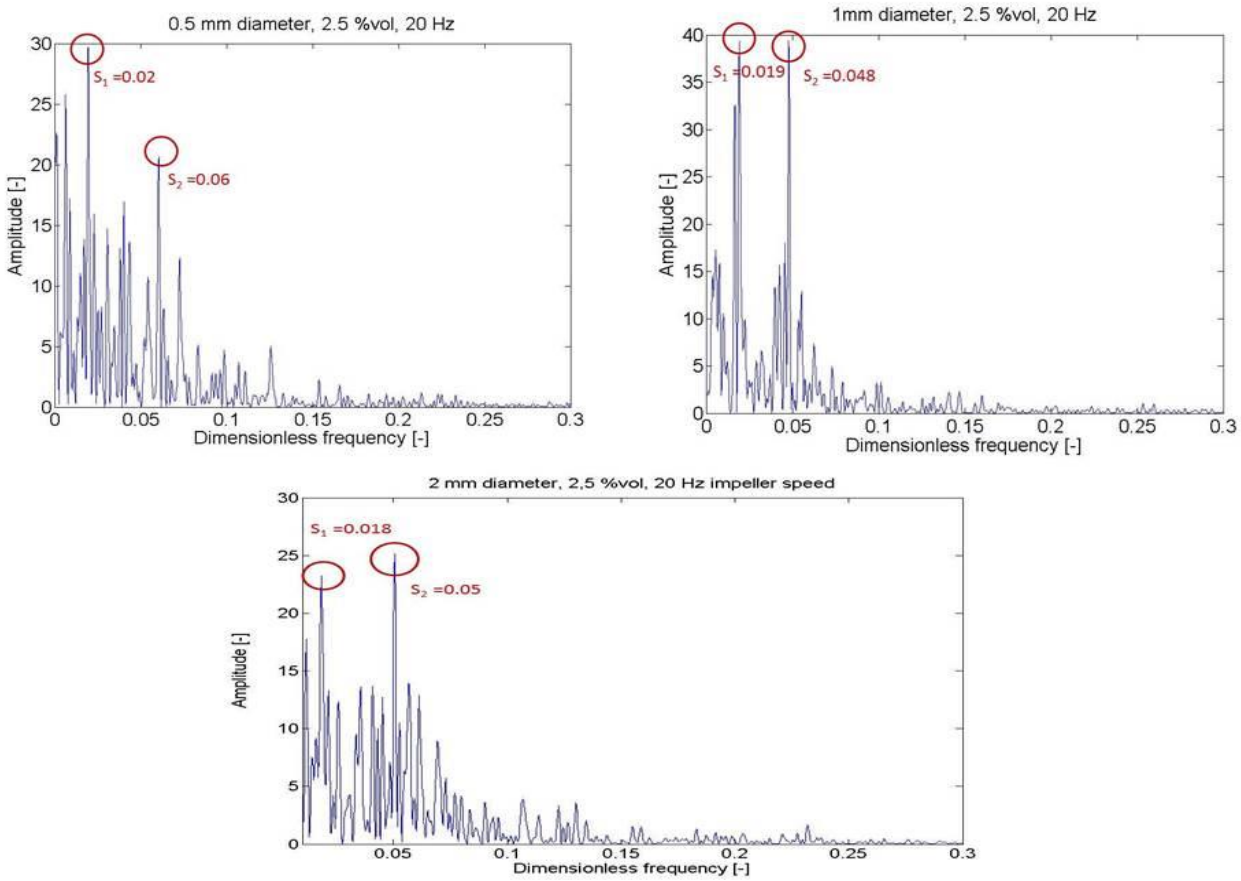

Figure 3.11: The Strouhal number and energy of S_1 and S_2 for the different particle sizes used in the experiments

3.3 CFD Simulation

The longest series of data is gathered from case 3 in Table 2.3 and represented approximately 4.4 seconds of real-time mixing. The shortest is gathered from case 4 which only covers 1.7 seconds of real-time mixing. Low simulation time gives a high uncertainty in the results. Comparing 4.4 seconds of simulation with 30 seconds of experimental data a frequency peak of 1.4 Hz will only record 6.2 periods in the simulations while 42 periods will be recorded in the experimental part. Quantitative data for this type of study comes from observation time rather than the number of studies. The results from the simulations have lack of accuracy due to the simulation time but they still show some consistency when comparing it to the experiments. For each CFD case, dominant frequencies appear which are within the low frequency periodicity and most cases managed to detect at least one peak comparable to the experiments.

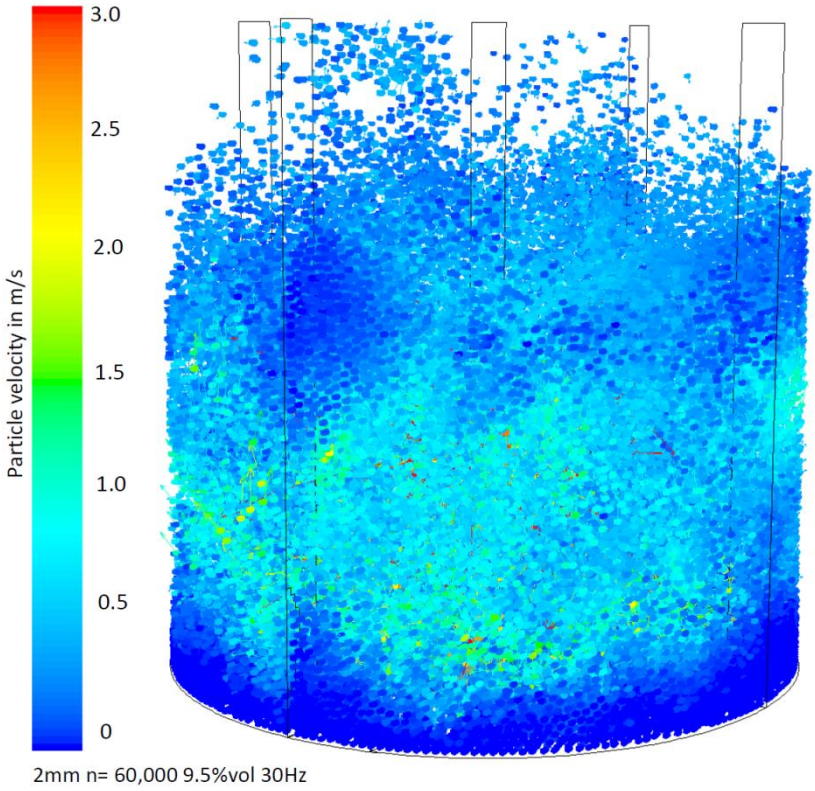

Figure 3.12: Instantaneous particle distribution from the simulations. The difference between the diluted region and the dense region can be detected as clearly in the simulations as in the videos from the experiments. This figure is taken from case 4.

The highest period detectable in the simulations are of 250 Hz which corresponds to a Strouhal number of 8.3 for case 2-4 and 12.5 for case 1. In figure 3.13 the energy spectrum is shown for all simulation cases. The energy spectra of the particles can be compared with the energy spectrum for continuous phase in figure 1.1. There is a similarity in the sense that most energy is found in the low periodic frequency however the figures are from different locations in the vessel and differences in the energy spectrum should exist. The impeller frequency and higher modes of the impeller frequency is not visible in the particle behavior far from the impeller. The energy spectrum for case 3 and case 4 show peaks close to S=1 which would indicate that the particles are directly following the impeller frequency.

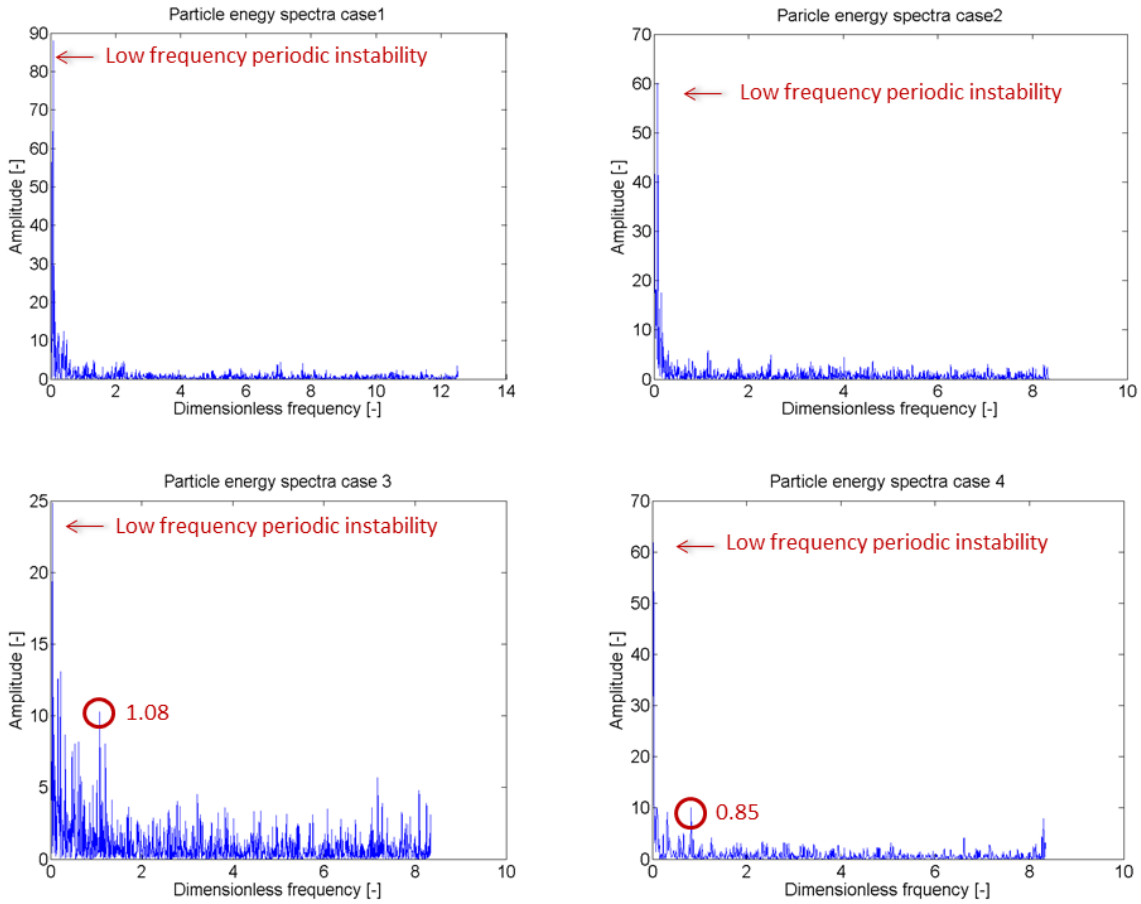

Figure 3.13: For all four cases the low frequency periodic instability is dominating the particle behavior. In case 3 and case 4 a peak close to S=1 appears which would imply that the particles are directly following the impeller speed.

In figure 3.14-3.17 the energy spectra from the height analysis in the simulations are shown. Case 2 differs a lot from the experimental results while the others are more similar. Due to the short simulation time the results are still not significant for the simulations.

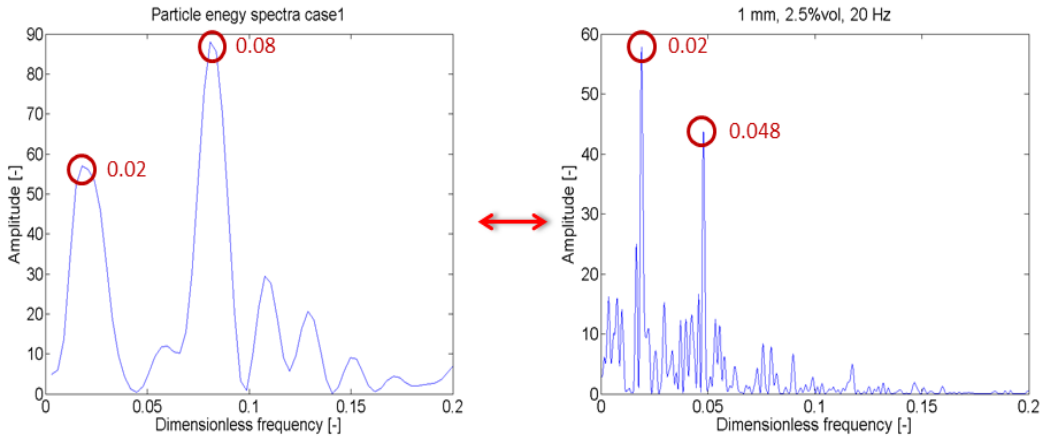

Figure 3.14: The energy spectra from the cloud height analysis of the simulations of case 1. Two dominant peaks appear in the simulations. One with a Strouhal number of 0.02 and on with 0.08.

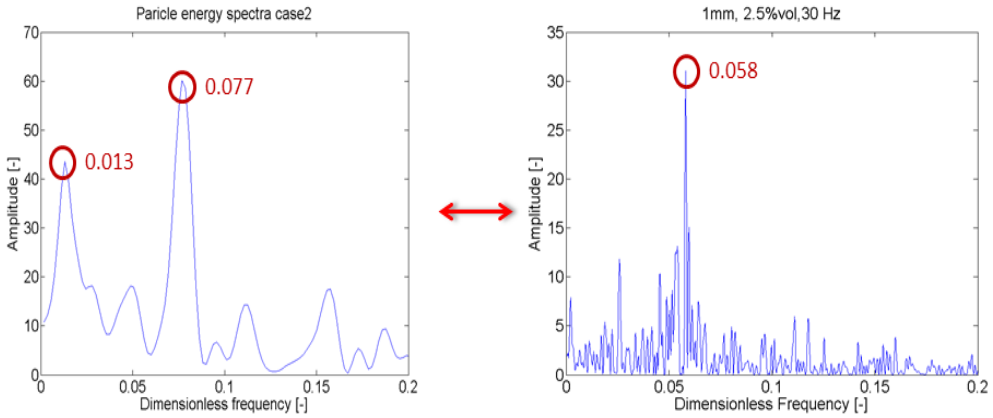

Figure 3.15: The energy spectra of simulation case 2. Two dominant peaks appear Strouhal numbers of of 0.013 and 0.077. The corresponding experimental case is at S=0.058 which is not far off.

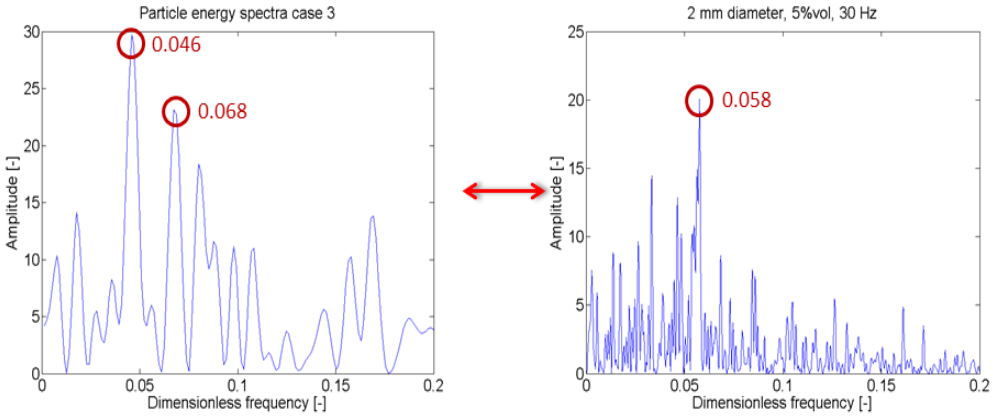

Figure 3.16: The energy spectra of simulation case 3. Two dominant peaks appear with Strouhal numbers of 0.046 and 0.068. These peaks are not far off from the experimental case with S=0.058.

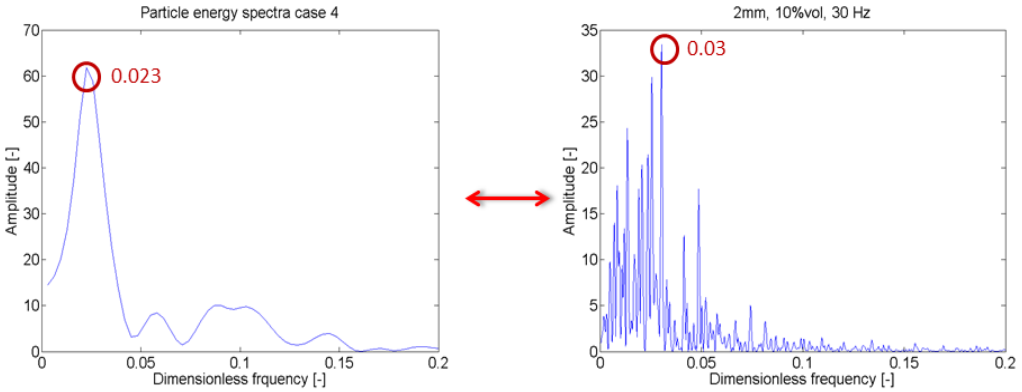

Figure 3.17: The energy spectra of simulation case 4. A peak appears at S=0.023 which similar to S=0.03 for corresponding experimental case.

4. Conclusions

The methods used to analyze the height and dynamics of the particle cloud prove good results. Both methods used for the experimental data show similar results and the method used for the simulations show all fundamental behaviors in a mixing vessel but with less accuracy.

Two dominant frequencies in the particle cloud which are referred to as S_1 and S_2 are detected. S_1 has a Strouhal number in the interval of 0.015-0.03 and S_2 has a Strouhal number in the interval of 0.045-0.06. S_2 is on the same level as the MI in the continuous phase and is therefore likely to be governed by the MI. S_1 exists as an energy containing frequency for all particle loadings while the energy of S_2 weakens with increased particle loading. These energy containing frequencies are constant with the Reynolds number of the continuous phase and particle sizes. Different behavior could be seen over the mixing vessel. On the windward side of the baffle both S_1 and S_2 were clearly dominant in the energy spectrum while on the leeward side of the baffle S_1 mainly dominated.

The energy fraction of the periodic behaviors of the particles is constant with impeller speed and particle diameter. For high volume fraction the amplitude of S_2 decreased while the energy for S_1 increased slightly. An unchanged energy fraction means that the forces generating the periodic behavior remain the same.

The post-processing of the particle cloud shows that the average height is linearly dependent of both Reynolds number and particle volume fraction. For increasing Reynolds number the average height increases linearly and for an increasing volume fraction the average height deceases linearly. The average height increases as the particle diameter decreases. However, the diameter does not show linearly dependence of the average height as for the Reynolds number and volume fraction. The method for determining the height is limited to one location and gives no further information for the detailed cloud height over the whole vessel. The standard deviation of the cloud height shows dependency of particle diameter. As the size of the particles decreases the cloud height variance will also decrease.

5. References

[1] M. Jahoda, M. Mostek and I. Fort, "CFD simulation of free liquid surface motion in a pilot plant stirred tank," *The Canadian Journal of Chemical Engineering,* vol. 89, no. 4, pp. 717-724, 2011.

[2] Z. Doulgerakis, M. Yianneskis and A. Duccin, "On the interaction of trailing and macro-instability vortices in a stirred vessel-enhanced energy levels and improved mixing potential," *Chemical Engineering Reaserch and Design,* vol. 87, no. 4, pp. 412-420, 2009.

[3] S. Roy, . S. Acharya and . M. D. Cloeter , "Flow structure and the effect of macro-instabilities in a pitched-blade stirred tank," *Chemical Engineering Science,* vol. 65, no. 10, pp. 3009-3024, 2010.

[4] M. Eng and A. Rasmuson, "Influence of soilds on macro-instabilities in a stirred tank," *Chamical Engineering Research and Design,* vol. 90, no. 8, pp. 1052-1062, 2012.

[5] K. Bittorf and S. Kresta, "Prediction of cloud height for solid suspensions in stirred tanks," *Chemical Engineering Research and Design,* vol. 81, no. 5, pp. 568-577, 2003.

[6] R. Chanaud, "Observations of oscillatory motion in certain swirling flows," *Journal of Fluid Mechanics,* vol. 21, no. 1, pp. 111-127, 1965.

[7] L. Nikiforaki, G. Montane and K. Lee, "On the origin, frequency and magnitude of macro-instabilities of the flows in stirred vessels," *Chemical Engineering Science,* vol. 58, no. 13, pp. 2937-2949, Issue.13 Vol.58 2003.

[8] P. Petersson and M. Aldén, "Lund University," Lund University, 13 11 2012. [Online]. Available: http://www.forbrf.lth.se/english/research/measurement_methods/laser_based_velocity_measurement_techniques_ldv_and_piv/. [Accessed 12 06 2014].

[9] P. Hasal, J. Montes and H. Boisson, "Macro-instabilities of velocity field in stirred vessel:: detection and analysis," *Chemical Engineering Science,* vol. 55, no. 2, pp. 391-401, 2000.

[10] L. Nikiforaki, "On the variation of precessional flow instabilities with operational parameters in stirred vessels," *Chemical Engineering Journal,* vol. 3, no. 217-231, p. 102, 2004.

[11] T. Zwietering, "Suspending of solid particles in liquid by agitators," *Chemical Engineering Science,* vol. 8, no. 3-4, pp. 244-253, 1958.

[12] A. Brucato, G. Micale, F. Grisafi and L. Rizzuti, "CFD simulation of particle suspension height in stirred vessels," *Chemical Engineering Research,* vol. 82, no. 9, pp. 1204-1213, 2004.

[13] W. Press, S. Teukolosky, W. Vetterling and B. Flannery, Numerical recipes in C, Cambridge: Cambridge University Press, 1999.